Sequence-controlled polyhydroxyurethanes with tunable regioregularity obtained from sugar-based vicinal bis-cyclic carbonates

Victor Salvado,[1,2] Marc Dolatkhani,[2] Étienne Grau,[1,*] Thomas Vidil,[1,*] Henri Cramail[1,*]

[1]Univ. Bordeaux, CNRS, Bordeaux INP, LCPO, 16 Avenue Pey-Berland, 33600 Pessac, France

[2] *PolymerExpert, 1 Allée du Doyen Georges Brus, 33600 Pessac, France*

Abstract

The carbonation of biosourced 1,2-diols is a sustainable avenue for the synthesis of bis(5-membered cyclic carbonate)s (bis-5CC), the precursors of a valuable class of polymers, *e.g.* polyhydroxyurethanes (PHUs). In this work, we performed the direct carbonation of optically pure sugar-based butadiene tetraols, namely (i) *meso*-erythritol and (ii) its *(S,S)* diastereoisomer, *(L)*-threitol. The corresponding vicinal bis-5CC, erythritol dicarbonate (EDC) and threitol dicarbonate (TDC) respectively, retain the stereochemistry of the starting tetraols. The comprehensive study of their aminolysis reaction, in DMSO and at room temperature, indicates that the kinetics and the regio-orientation of the ring opening of the 5CC are very dependent on their stereochemistry. The total aminolysis of EDC results in the formation of hydroxyurethanes with an excess of secondary hydroxyl groups, $(OH)_{II}$, of about 85%, against 60% for TDC. Moreover, when considering the two consecutive aminolyses of EDC (resp. TDC), the kinetic rate constant of the first aminolysis $k_{1,EDC}$ (resp. $k_{1,TDC}$) is one order of magnitude higher than that of the second aminolysis, $k_{2,EDC} \sim k_{1,EDC}/10$ (resp. $k_{2,TDC} \sim k_{1,TDC}/10$). We used this feature to develop a one-pot, two-step polymerization procedure offering sequence-controlled PHUs. All the experimental results are well supported by DFT calculations. In the end, the comparative study of these two diastereoisomers of simple sugar-based vicinal bis-5CCs, provides a new family of PHUs with tunable sequence- and regio-regularity.

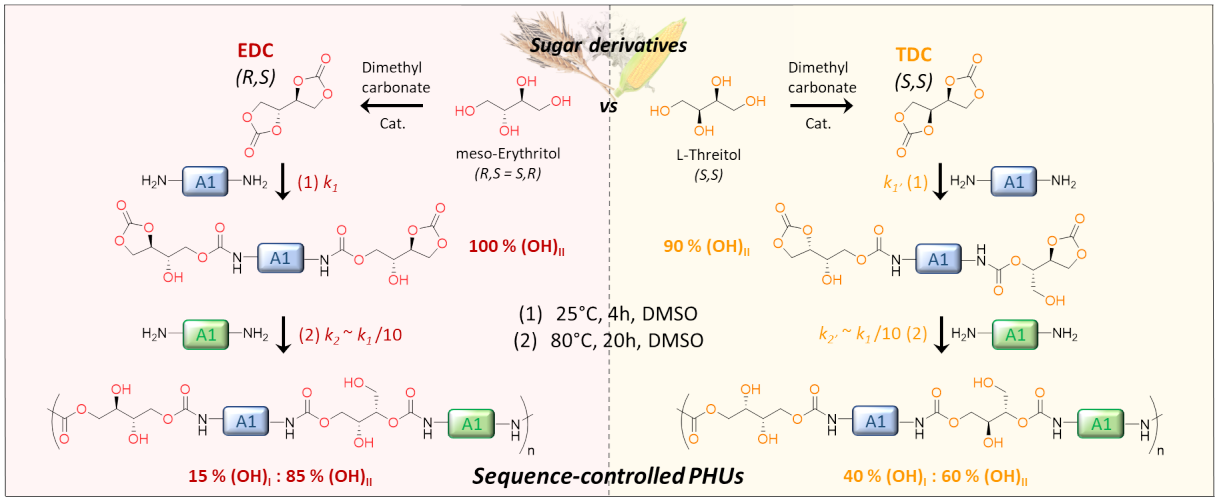

Introduction

Polyhydroxyurethanes (PHUs) are phosgene and isocyanate-free polyurethanes (PUs) that are foreseen as a promising alternative to conventional polyurethanes (PUs), when European and North American directives will restrict the use of allergenic and carcinogenic isocyanates. [1,2] They are usually obtained through the polyaddition reaction of diamines onto bis(5-membered cyclic carbonate)s (bis-5CC), resulting in the formation of urethane linkages and hydroxyl groups (OH) (scheme 1). The success of PHUs is largely related to the rapid development of sustainable procedures for the synthesis of 5CC precursors such as the CO_2/epoxide coupling chemistry [3–7] or the carbonation of biosourced 1,2-diols.[8–12] However, 5CC aminolysis comes with several drawbacks including (*i*) slow kinetics and extensive side reactions that hinder high polymerization degree [13–15] and (*ii*) a lack of regio- and stereo-control resulting in poorly defined polymers.[11,16] Many catalysts have already been proposed to accelerate the polymerization kinetics, including N-bases, metal salts and thiourea compounds.[17,18] While they accelerate the reaction, they currently do not solve the regio- and stereo-regularity issues. Yet, regularity in the arrangement of polymer backbones neighboring units is of paramount importance, as it is critical to their bulk performances. It includes their thermomechanical properties [19,20] but also, when it applies, their optoelectrical behavior [21] or their biodegradability.[22]

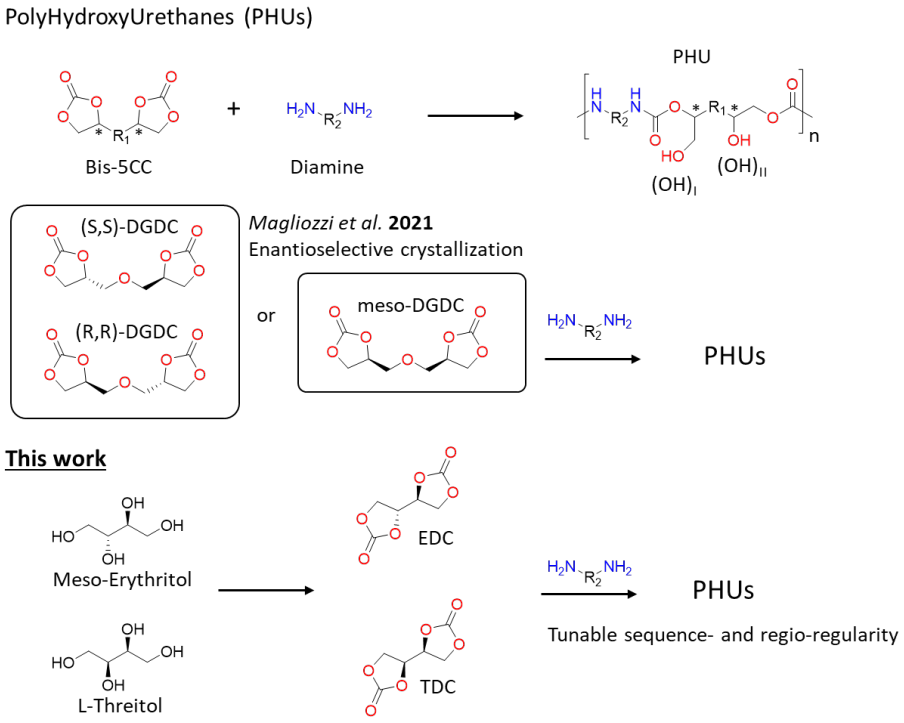

Scheme 1: General chemical equation for the synthesis of PHUs starting from Bis-5CCs and diamines. The methine carbon of Bis-5CC, marked with an asterisk (*), are stereocenters. Structure of the stereoisomers of DGDC used by Magliozzi *et al.* (2021), and structures of *meso*-erythritol and *L*-Threitol, and their corresponding Bis-5CCs: EDC and TDC respectively.

The lack of regiocontrol in the aminolysis of 5CC, *i.e.* the formation of mixtures of primary, $(OH)_I$, and secondary, $(OH)_{II}$, alcohols, is a general noted drawback for PHU synthesis.[16] Authors have tentatively addressed the problem by designing suitable monomers. Among them, the group of Endo *et al*. have demonstrated that the selectivity in favor of $(OH)_{II}$ formation can be increased by increasing the electron-withdrawing ability of the α- or β-substituents of the 5CC.[23–25] More recently, Kleij *et al.* have demonstrated that 5CC with bulky substituents can be ring-opened under organocatalytic control (*e.g.* TBD) with a regioisomer excess up to > 99% (*e.g.* $(OH)_{II}$).[26] However, to the best of our knowledge, all these methods were tested with model molecules. The preservation of the regiocontrol during the polymerization of bis-5CC derived from these model molecules has not been confirmed yet. More importantly, there are no existing methods to control the degree of regioregularity for the polymerization of a given bis-5CC structure, and thus to explore the impact of the regioregularity on the properties of the resulting PHUs.

As for stereoregularity in PHUs synthesis, it is nearly unaddressed in the literature. This challenge is relegated to the background due to the prevalence of side reactions and low molar masses issues. Yet, the methine carbon of 5CC are stereocenters (Scheme 1) that are inserted in the polymeric chains derived from them.[11] Since the chirality of bis-5CC precursors is usually not controlled, their polyaddition with diamines results in stereo-irregular PHUs. To our knowledge, only one study explored the influence of the stereochemistry of a bis-5CC onto its reactivity and the properties of the resulting PHUs. It was recently reported by Magliozzi *et al*., who used a procedure of resolution by crystallization to isolate two crystal structures of diglycerol dicarbonate (DGDC, Scheme 1): the enantiopure *meso*-DGDC, *(R,S)*, and the racemic mixture of *(R,R)* and *(S,S)* DGDC.[10] These two crystals were polymerized in bulk with various diamines (110 °C). Interestingly, the characterizations of the resulting PHUs suggest a slight impact of the stereochemistry of DGDC on the chain insertion efficiency and on the regioregularity of the chains. PHUs derived from *meso*-DGDC exhibit slightly higher molar masses, while PHUs obtained from the racemic mixture of *(R,R)* and *(S,S)* DGDC come with higher contents of $(OH)_I$. Despite these intriguing results, the procedure to isolate the DGDC stereoisomers is tedious, preventing larger-scale synthesis and systematic studies.

Herein, we propose to use enantiopure bis-5CC obtained from the direct carbonation of sugar-based butadiene tetraols that are enantiopure themselves, namely (i) *meso*-erythritol and (ii) its *(S,S)* diastereoisomer, *(L)*-threitol (Scheme 1).[27] Recently, Dannecker and Meier introduced a simple and sustainable method for the organocatalytic carbonation of *meso*-erythritol in the presence of dimethyl carbonate used both as a reagent and a solvent.[8] The corresponding erythritol di(carbonate) (EDC) retains the stereochemistry of the starting tetraol and is obtained in very high yield (90%). We propose to apply the same procedure to *(L)*-threitol, to obtain a set of two optically pure stereoisomers of butadiene dicarbonates: EDC and its *(S,S)* diastereoisomer threitol di(carbonate) (TDC). The aminolysis of EDC and its use for the synthesis of PHUs is already well documented in the literature.[28–32] In particular, several authors reported the straightforward aminolysis of EDC in very mild conditions, including room temperature. This remarkable feature was attributed to the strong mutual inductive effect that the vicinal 5CC exert on each other.[31,33] However, to the best of our knowledge, there is no report regarding the quantitative measurement of the kinetics rate of the reaction. Schmidt *et*

al. valorized the very high reactivity of EDC for the synthesis of high molecular weight PHUs (M_n ~ 10 kg mol^{-1}) by melt-compouding (T ~ 80 °C - 100 °C), but the reactions are so fast under these conditions, that it is virtually impossible to study their kinetics.[31] Here, we perform a comprehensive study of the aminolysis reaction of EDC and TDC in solvent and at room temperature. The experimental results, supported by DFT calculations, indicate that the kinetics and the regio-orientation of the ring opening of the 5CC are very dependent on the stereochemistry of EDC and TDC respectively. Moreover, when considering the two consecutive aminolyses of EDC (resp. TDC), the kinetic rate constant of the first aminolysis $k_{1,EDC}$ (resp. $k_{1,TDC}$) is one order of magnitude higher than that of the second aminolysis, $k_{2,EDC}$ ~ $k_{1,EDC}$/10 (resp. $k_{2,TDC}$ ~ $k_{1,TDC}$/10). We use this feature to develop a one-pot, two step polymerization procedure offering sequence-controlled PHUs.[34] In the end, the comparative study of the two vicinal dicarbonates, *e.g.* EDC and TDC, provides a new family of PHUs with tunable sequence- and regio-regularity. The impact of the chain-regularity of the PHUs on their thermal properties is investigated.

1. Synthesis of EDC and TDC

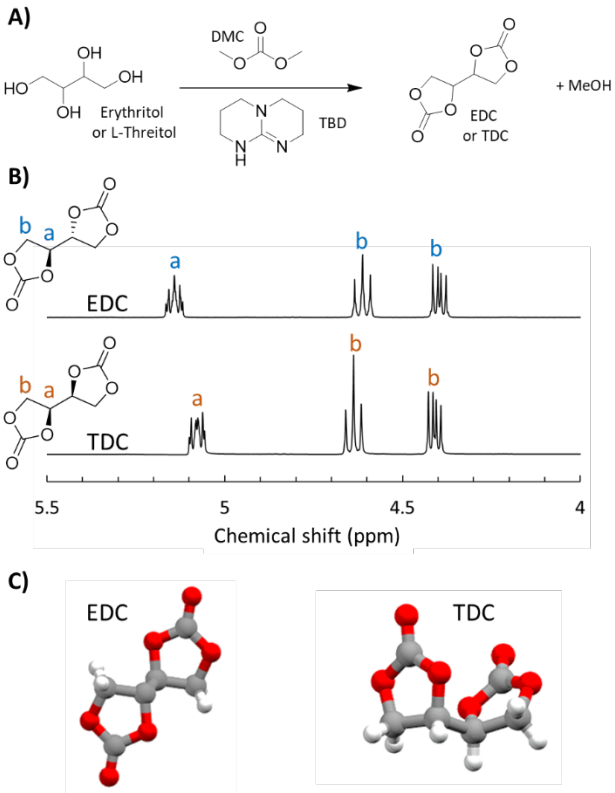

Figure 1: **A) Synthesis of erythritol dicarbonate (EDC) and L-threitol dicarbonate (TDC), by transesterification of erythritol and L-threitol respectively, with DMC using TBD as an organocatalyst. B) ^{1}H NMR spectra of EDC and TDC (DMSO-d_6). C) 3D representation of EDC and TDC molecules in their crystalline state obtained by X-ray crystallography of their corresponding single-crystal**.

In this work, erythritol di(carbonate) (EDC) was synthesized starting from *(R,S)* erythritol according to the procedure recently described by Dannecker and Meier [8] (Figure 1A, 84%

yield; additional experimental details, materials, and methods are available in the Supporting Information, SI). The same method was applied successfully to L-threitol, the *(S,S)* diastereoisomer of erythritol (93% yield). This is the first report of the synthesis of L-threitol di(carbonate) using this method. For sake of simplicity, it is called threitol di(carbonate) (TDC) in the rest of the paper. The structure of the two diastereoisomers was confirmed by NMR measurements (Figure 1B). Moreover, single-crystals of EDC and TDC were analyzed by X-ray crystallography, indicating that the *(R,S)* and the *(S,S)* isomers are both monoclinic crystals (Supporting information: crystal parameters for EDC and TDC, Figure S1). Figure 1C represents their tridimensional structure. The two carbonate cycles of EDC are located on either side of the butane skeleton, meaning that the carbonyl groups point in opposite direction in a *trans* conformation. In the case of TDC, the two carbonate cycles are facing each other in a *gauche* conformation. The crystallographic data confirm that the stereochemistry of the dicarbonates is consistent with those of the starting tetraols.
The melting temperature, T_m, of the two crystals were measured by Dynamic Scanning Calorimetry, DSC (Supporting information: DSC traces of EDC and TDC, Figure S2). The melting point of EDC, T_m = 169 °C, is higher than that of TDC's, T_m = 137 °C. These results confirm that the stereoisomery of bis(carbonate) impacts their thermal properties, as already noticed by Magliozzi *et al.* for the stereoisomers of DGDC.[10]

2. Study of the aminolysis of EDC at 25 °C in DMSO

The aminolysis of EDC in solution was succinctly investigated by Goldstein *et al*. in 1971.[28] The authors studied the reaction of EDC with butylamine (BA) at 50 °C in DMF (0.2 mol.L^{-1}), using NMR spectrometry. For [BA] = 2[EDC] (*i.e.* [NH_2] = [CC] where CC = cyclic carbonate), they observed that the reaction follows a second kinetic order up to a conversion of ~ 47% for the global CC functions. Then the reaction stops. It was assumed that after the ring opening of one of the two CC of EDC, the remaining CC was unreactive. This assumption was based on the hypothesis of the mutual influence of the vicinal CC units that exert a strong inductive effect on each other. This effect fades away after the first ring opening, and the remaining CC is much less reactive. Their hypothesis was supported by theoretical calculations of the kinetic rate constant of the CC aminolysis, which was found to be in close agreement with experimental results. However, the structure of the product obtained after the first ring opening reaction was not elucidated and the second ring opening reaction was not studied at all.

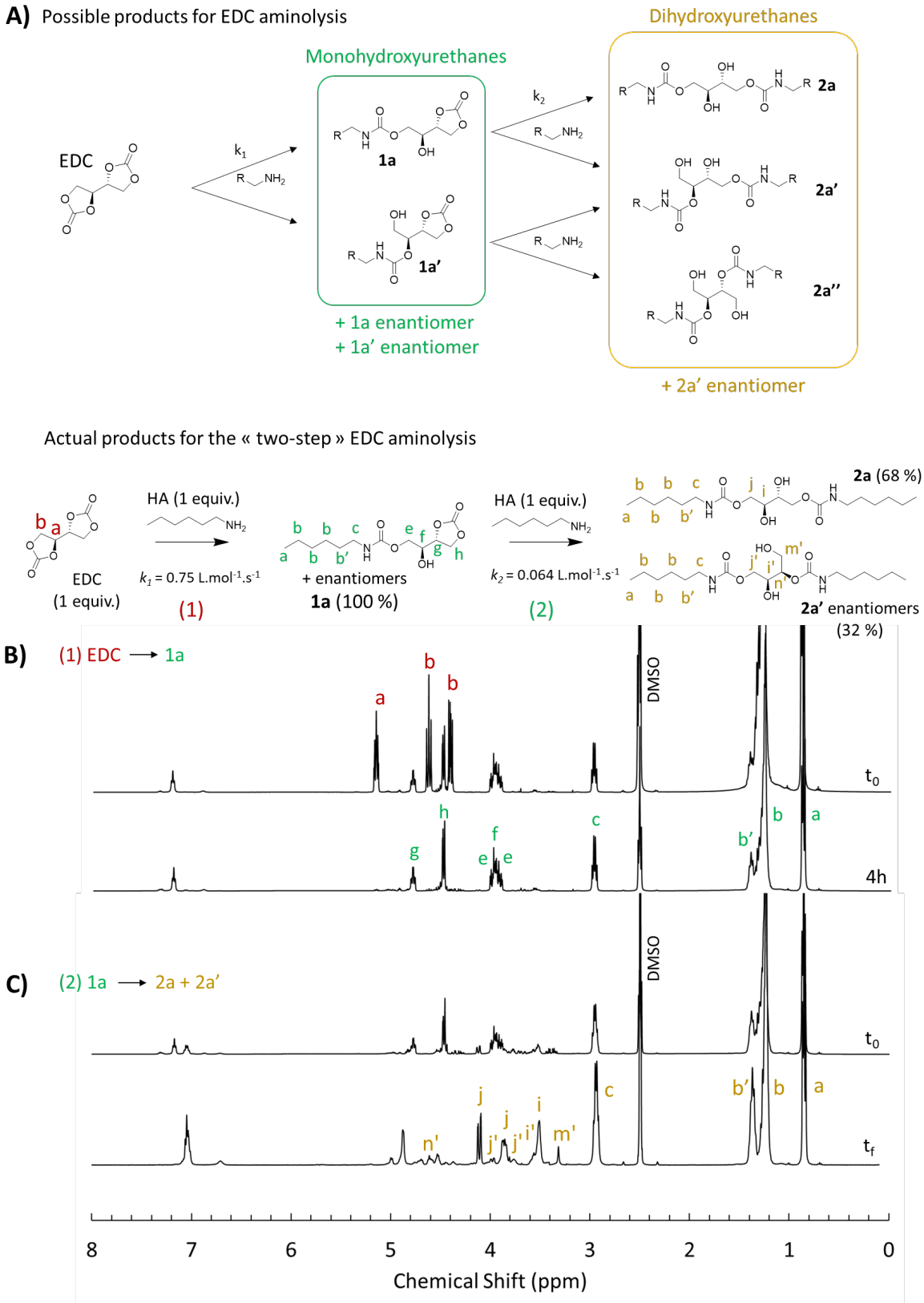

Figure 2: A) Possible products for EDC aminolysis and actual products obtained in this work for the "two-step" EDC aminolysis. B) ^{1}H NMR spectra for the reaction of EDC (1 equiv.) with hexylamine (1 equiv.) at t_0 and after t = 4 h (DMSO-d_6). C) ^{1}H NMR spectra for the reaction of 1a (1 equiv.) with hexylamine (1 equiv.) at t_0 and after t_f = 2 weeks. (DMSO-d_6).

In the present study, EDC was first reacted with 1 equiv. of hexylamine (HA) in DMSO ([EDC] = 1 mol.L^{-1} and [NH_2] = 1/2[CC]) at 25 °C. As shown in Figure 2A, many products can be expected depending on the chemo- and the regio-selectivity of the reaction. Mono- (**1a**, **1a'**) and/or di-hydroxyurethanes (**2a**, **2a'**, **2a''**) can be obtained depending on whether only one or two of the CC functions of EDC are involved in the reaction. Moreover, the mono- and di-hydroxyurethanes can be made of primary, $(OH)_I$, and/or secondary alcohols, $(OH)_{II}$, depending on the regioselectivity of the ring opening additions. The reaction progress was monitored by ^{1}H NMR spectroscopy (Supporting information: kinetics of EDC aminolysis, Figure S3). Figure 2B represents the NMR spectra of the crude at t = 0 and after t = 4 h of reaction. The proton signals **a** and **b** of EDC decreases rapidly, while new signals **g**, **h**, **e**, **f** and **c** increases concomitantly. Further analyses of the crude obtained after 4 h of reaction (Supporting information: ^{13}C, ^{1}H-^{1}H COSY and ^{1}H-^{13}C HSQC NMR spectra of all compounds, Figures S4 to S7) indicate that these new signals are attributed to the protons of the mono-hydroxyurethane **1a** (presumably existing in the form of two enantiomers, *(R,S)* and *(S,R)*, that cannot be distinguished on the NMR spectra). The integrals indicate that EDC is quantitatively transformed into **1a**. Thus, the reaction is 100% chemoselective, with only one of the two CC functions of EDC being ring-opened. This result is in accordance with the prediction of the seminal work of Goldstein *et al.*[28] Interestingly, the reaction is also regiospecific, *i.e.,* the ring opening reaction results in the formation of $(OH)_{II}$ exclusively. Examples of such selectivity in the regiocontrol of the uncatalyzed aminolysis of CC are extremely rare. As far as we know, only two reports show complete regiocontrol in the uncatalyzed aminolysis of 5-members CC. They were both reported by the group of Endo *et al*. for the aminolysis of α-trifuoromethyl [23] and β-chloro-substituted [24] CC. The same group demonstrated that the selectivity in favor of $(OH)_{II}$ formation increased as the electron-withdrawing ability of the α- or β-substituent increases. Based on these results, they stated that the direction of the ring-opening aminolysis of 5-membered CC can be controlled by the electronic effect of substituent introduced on the carbonate ring. Thus, the regiospecificity observed for the aminolysis of EDC is in accordance with the strong mutual inductive effect that the vicinal CC units exert on each other.

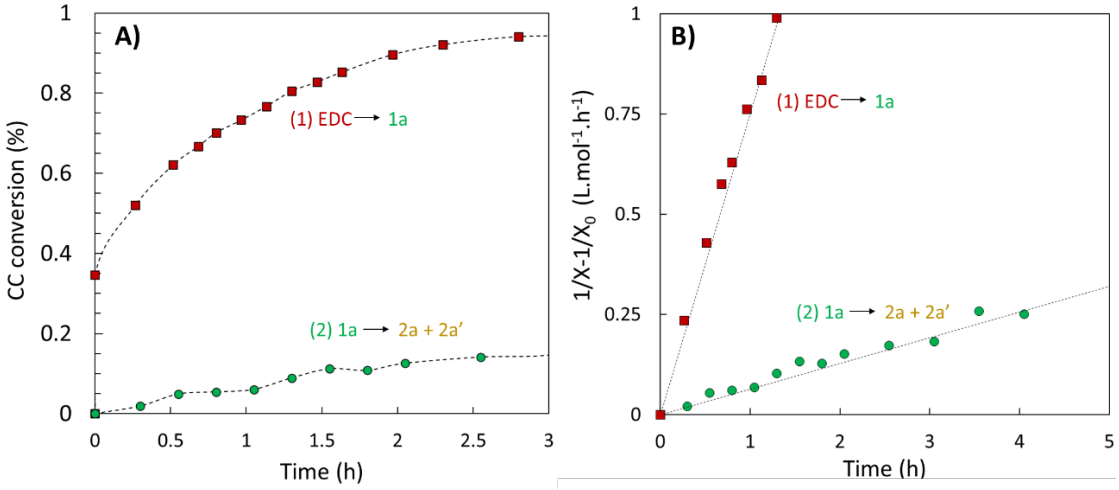

Figure 3: A) Conversion of EDC into 1a as a function of time measured by ^{1}H NMR monitoring for the reaction of EDC (1 equiv.) with hexylamine (1 equiv.) (red points) and conversion of 1a into 2a and 2a' for the reaction of 1a (1 equiv.) with hexylamine (1 equiv.) (green points) (T = 25

°C). B) Corresponding plots of $1/X-1/X_0$ as a function of time, where X is the concentration of EDC for the red points and 1a for the green points. The linear plots indicates that the reactions are second-order reactions. The slope of the plots provides the second-order rate constants, $k_{1,EDC}$ and $k_{2,EDC}$, for the reactions of EDC with hexylamine and 1a with hexylamine respectively.

Figure 3A represents the evolution of the conversion of EDC into **1a** (red plot) as a function of time. The slope of the corresponding second-order plot (Figure 3B, red plot) indicates that the second-order rate constant $k_{1,EDC}$ of the ring-opening reaction of EDC is equal to 0.75 $L.mol^{-1}.h^{-1}$. To our knowledge, very few kinetic rate constants have been measured at 25 °C for the aminolysis of 5-membered cyclic carbonate, because these ring-opening additions are usually very slow close to room temperature. Only 5-membered CC activated by very strong electron withdrawing substituent can display a significant aminolysis rate at room temperature. Our group measured a kinetic rate constant, k_{ester}, of about 0.42×10^{-4} $L.mol^{-1}.h^{-1}$ at 25 °C for the ring opening addition of HA onto a strongly activated CC with an ester as β-substituent (DMSO, 1 $mol.L^{-1}$).[15] The kinetic rate constant of the first ring opening of EDC is much larger, $k_{1,EDC} \sim 10^4 \times k_{ester}$, illustrating once again the strong mutual activation of the vicinal CC units.
In order to study the subsequent ring-opening aminolysis of the *in-situ* generated mono-carbonate **1a**, an additional equivalent of HA was added to the reaction mixture. Again, the reaction progress was monitored by ^{1}H NMR spectroscopy at 25 °C by monitoring the progress of the integral of signal **h** (Supporting information: ^{1}H NNR kinetics of **1a** aminolysis, Figure S8). The green plot of Figure 3A indicates that the conversion of CC is much slower this time. The second-order rate constant k_2 was calculated to be 0.064 $L.mol^{-1}.h^{-1}$, *i.e.,* $k_{2,EDC} \sim k_{1,EDC}/10$. The reaction was brought to completion by increasing the temperature to 60 °C for a total of 4 hours. The NMR analyses of the crude indicate that both the **2a** and **2a'** compounds are formed (Figure 2C and Supporting information: ^{13}C, ^{1}H-^{1}H COSY and ^{1}H-^{13}C HSQC NMR spectra of all compounds, Figures S9 to S12). Indeed, 16% of the overall hydroxyl groups in the crude are $(OH)_I$, indicating that **2a'** was formed. The ratio of the two regioisomers was calculated to be **2a**:**2a'** = 68:32. Thus, the second ring opening addition is not regiospecific, however there is a significant orientation of the regiocontrol in favor of $(OH)_{II}$ formation.

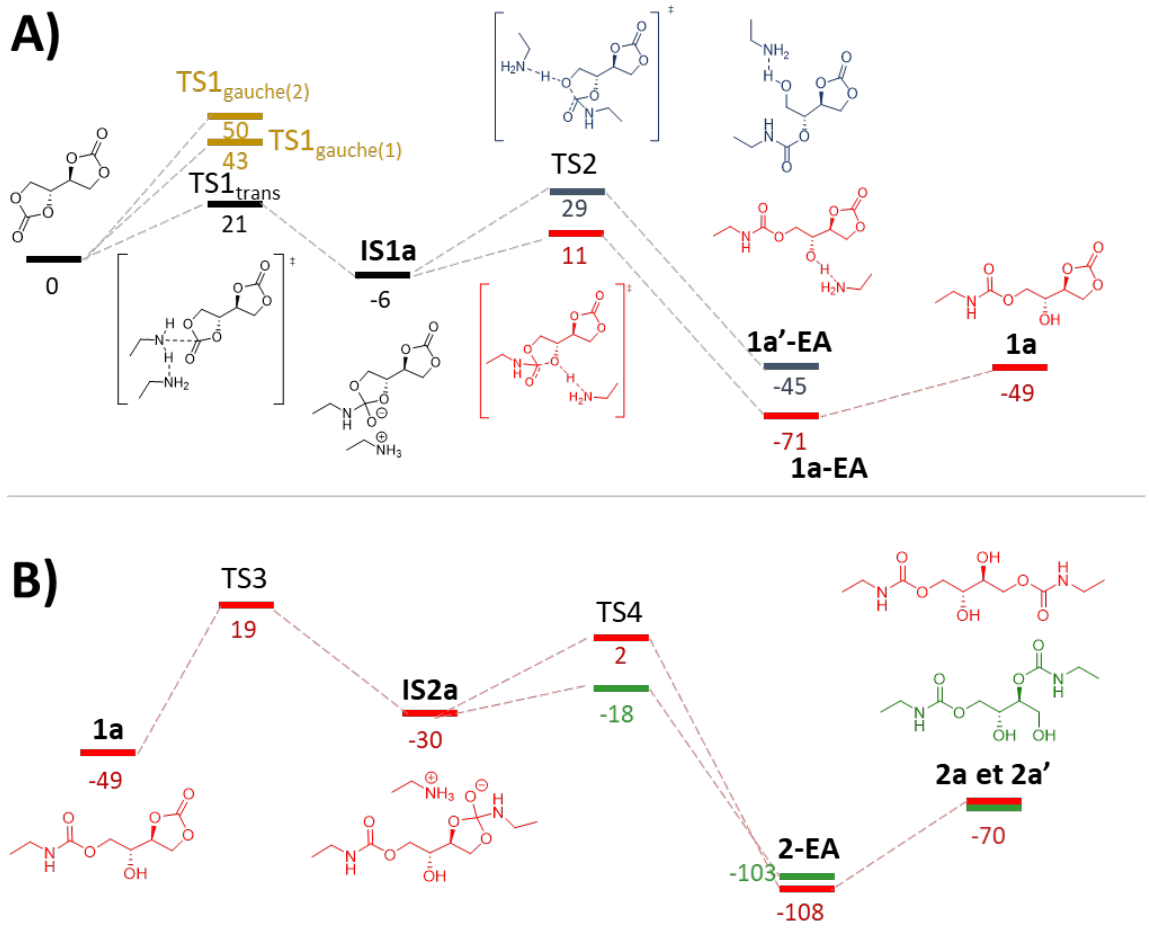

Figure 4: A) Energy levels of transition states (TS) and intermediate states (IS) of EDC aminolysis in presence of ethylamine (EA). Note: the calculation for the whole mechanistic pathway were done for EDC being in *trans* conformation. For the rate determining step, *i.e.* the transformation of EDC into IS1A, the calculation were also performed for the *gauche* conformers of EDC. The energy levels of the corresponding transition states, $TS1_{gauche(1)}$ and $TS1_{gauche(2)}$, are indicated in brown colour. B) Energy levels of transition states (TS) and intermediate states (IS) of 1a aminolysis in presence of ethylamine (calculations for the *trans* conformation of 1a). The Gibbs free energies are expressed in kJ.mol^{-1}. (DFT-BP86 def2-SVP, DMSO, 25 °C, [CC] = [EA], non-concerted mechanism and self-catalysed by EA)

The experimental results were compared to mechanistic DFT calculations. Preliminary calculations, (Supporting Information: ORCA calculations for the aminolysis of propylene carbonate, Figure S13), indicate that the overall reaction proceeds according to a non-concerted mechanism, self-catalysed by the amine, in accordance with previous reports of the literature. Figure 4A represents the mechanistic pathways for the first aminolysis of EDC, using ethylamine as a model of hexylamine for sake of simplicity. The initial step corresponds to the nucleophilic attack of the amine onto the carbonate group of CC accompanied by a proton transfer towards the catalytic amine to provide a cyclic amino alkoxide anion interacting with NH_3^+ by H-bonding, **IS1A**. It subsequently undergoes ring opening by C–O bond cleavage and a simultaneous proton transfer between NH_3^+ and the O atom of the carbonate to produce the monohydroxyurethanes interacting by H-bonding with the catalytic amino function, **1a-EA** and **1a'-EA**, where EA stands for the catalytic ethylamine interacting with the two regioisomers at

the end of the reaction. Clearly, **1a-EA**, the $(OH)_{II}$ containing regioisomer, is much more stable than **1a'-EA**, $\Delta(\Delta G)$(**1a'-EA**–**1a-EA**) = 26 kJ.mol^{-1}, indicating that the formation of this regioisomer is thermodynamically favorable. Moreover, the energy difference between the intermediate species, **IS1A**, and the transition state, **TS2**, is much smaller in the case of the mechanistic pathway resulting in the formation of **1a-EA** ($\Delta(\Delta G^{\neq})$ = 18 kJ.mol^{-1}). Thus, the formation of **1a-EA** is also kinetically favorable. Overall, the calculations are in accordance with the regiospecificity of the reaction observed experimentally, both under thermodynamic and kinetic control. The dihydroxyurethanes **2a** and **2a'** are obtained according to the same mechanistic pathway (Figure 4B). However, the energy difference between the two regioisomers is much smaller this time, $\Delta(\Delta G)$(**2a'-EA**–**2a-EA**) = 5 kJ.mol^{-1}, suggesting a moderated regioselectivity in favor of **2a** formation under thermodynamic control. When considering the energy difference between the intermediate species, **IS2A**, and the transition state, **TS4**, the formation of **2a'** is much more favorable ($\Delta(\Delta G^{\neq})$ = 20 kJ.mol^{-1}). Experimentally, **2a**:**2a'** = 68:32, indicating that the regio-orientation of the reaction is in accordance with a thermodynamic control.

3. Study of the aminolysis of TDC at 25 °C in DMSO

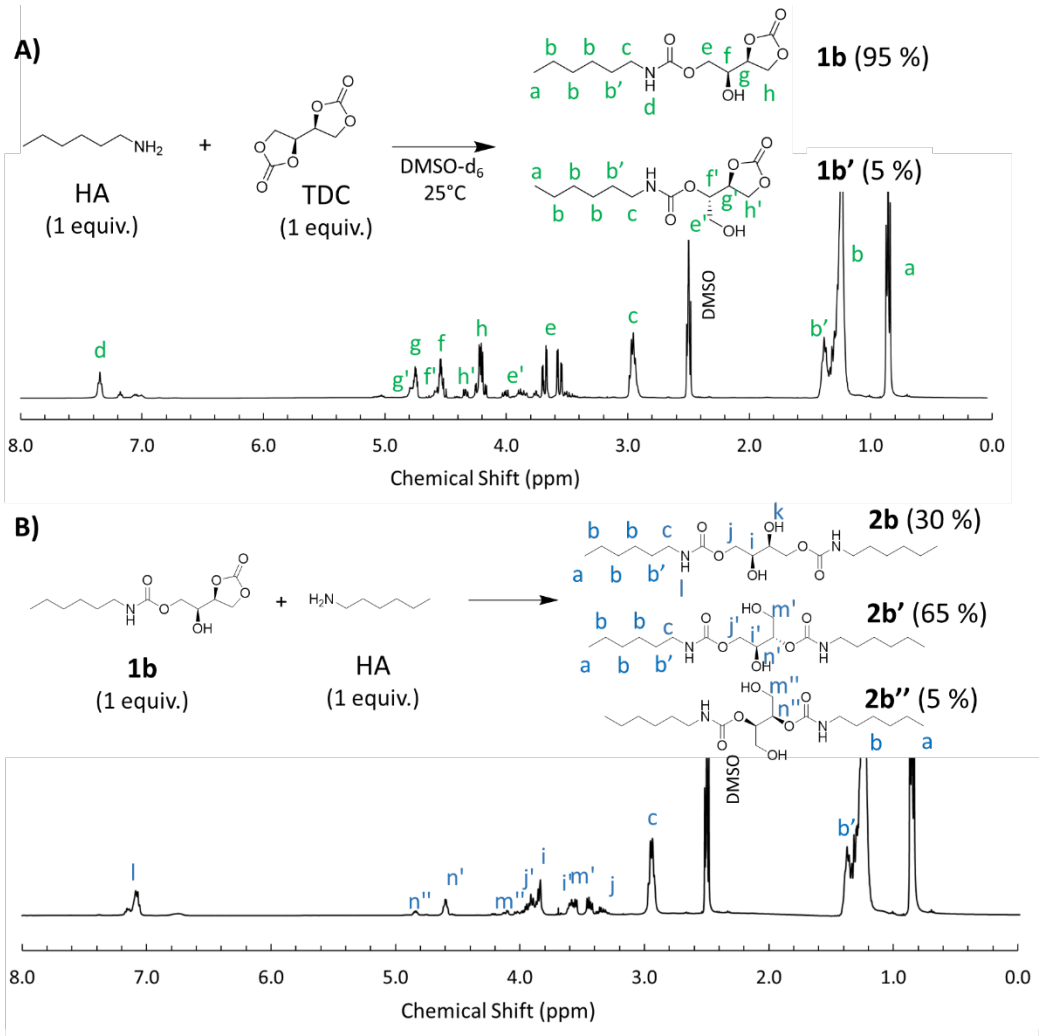

Figure 5: A) ^{1}H NMR spectrum (DMSO-d_6) of the mixture of 1b (95%) and 1b' (5%) obtained after the aminolysis of TDC (1 equiv.) in presence of HA (1 equiv.). B) ^{1}H NMR spectrum of the mixture of 2b, 2b' and 2b'' obtained after the aminolysis of the mixture of 1b (95%) and 1b' (5%) in presence of HA (1 equiv.).

The aminolysis of TDC was studied according to the same protocol as EDC. It was first reacted with 1 equiv. of HA in DMSO at 25 °C ([TDC] = 1 mol.L^{-1} and [NH_2] = 1/2[CC]). The NMR analyses of the crude indicate that the reaction is chemoselective with only mono-hydroxyurethanes being formed (Figure 5A and Supporting information: ^{1}H, ^{13}C, ^{1}H-^{1}H COSY and ^{1}H-^{13}C HSQC NMR spectra of all compounds, Figures S14 to S18). Moreover, there is a strong regio-orientation in favor of **1b** formation, the $(OH)_{II}$ containing regioisomer. However, contrarily to EDC, the reaction is not regiospecific, the regioisomer **1b'** is also formed to a small extent, with **1b** : **1b'** = 95 : 5. This result indicates a very small impact of the stereoisomery of the vicinal dicarbonate on the regioselectivity of the first aminolysis.
The second-order rate constant $k_{1,TDC}$ of the ring-opening reaction of TDC is equal to 0.31 L.mol^{-1}.h^{-1} (Supporting information: kinetics constant of EDC and TDC aminolysis, Figure S19). This value is high as compared to the values reported in the literature for the aminolysis of activated CC (cf. $k_{ester} = 0.42\times10^{-4}$ L.mol^{-1}.h^{-1} at 25 °C).[15] However, it is significantly smaller than $k_{1,EDC}$ ($\sim k_{1,TDC}\times2$) indicating an influence of the stereoisomery of the vicinal dicarbonate onto the first-aminolysis kinetics. Goldstein *et al*. already noticed the influence of stereoisomery onto the kinetics of the aminolysis of carbonated hexitol, *i.e.* vicinal tricarbonates (50 °C, DMF).[28] The second-order rate constant of the first aminolysis varied according to the following order: isotactic > heterotactic > syndiotactic. They suggested that the evolution might be due to variation of steric factors resulting from different conformational isomerism of the vicinal tricarbonates. Based on this hypothesis, we tentatively used DFT calculation to predict the conformational analysis of EDC and TDC, *i.e.* the study of the relative energy between their different conformations. Figure 6 represents the relative conformation energy diagram of both EDC and TDC in DMSO at 25°C, as a function of the torsion angle, θ, between the half-planes π_A and π_B, where π_A is defined by O_1, C_3 and C_2 and π_B is defined by O_4, C_2 and C_3 (Figure 6). The energy diagram of EDC exhibits a conventional profile with two local minima for θ = 65°and 295°, corresponding to *gauche*-conformers and one absolute minimum, for θ = 180°, corresponding to the *trans*-conformer. The calculation of the population distribution according to a Boltzmann distribution, indicates that 92% of the molecules are in the *trans* conformation in agreement with the X-ray structure of the single-crystal (see Figure 1C). In this conformation, the two carbonyl groups point in opposite direction and they are easily accessible for aminolysis. It is worth noting that the mechanistic DFT calculations reported in Figure 4A for the aminolysis of EDC were performed by considering the *trans* conformer of EDC (θ = 180°). If the same calculations are performed with the *gauche* conformer, θ = 65° (or θ = 295°), then the barrier heights of the rate-determining step of the aminolysis, *i.e.* the formation of the transition state TS1, is drastically increased from 21 kJ.mol^{-1} to 50 kJ.mol^{-1} (or 43 kJ.mol^{-1} for θ = 295°), indicating that the reaction becomes kinetically unfavorable. This is well illustrated by representing the energy level of the corresponding transition states associated to the *gauche* conformers, $TS1_{gauche(1)}$ (θ = 65°) and $TS1_{gauche(2)}$ (θ = 295°), in Figure 4A. The relative conformation energy diagram of TDC exhibits three local energy minima as well, for θ' = 60°,

170° and 295°. However, the relative free energy of the *gauche* conformer associated to $\theta' = 295°$ is very close to those of the *trans* conformer ($\theta' = 170°$). The calculation of the population distribution indicates that 73% of the molecules are in the *gauche* conformation (also in agreement with X-ray results) and 27% in the *trans* conformation (DMSO at 25 °C). Similarly to EDC, the mechanistic DFT calculations indicate that the aminolysis of the *gauche* conformers of TDC is kinetically unfavorable (Supporting information: ORCA calculations for TDC aminolysis, Figure S25). Since only 27% of TDC molecules are in the *trans* conformation, against 92% for EDC, then the kinetics of TDC aminolysis is expected to be much slower than EDC aminolysis. Thus, the conformational analysis of EDC and TDC is consistent with the higher aminolysis rate of EDC observed experimentally by NMR (*i.e.* $k_{1,EDC} \sim k_{1,TDC} \times 2$).

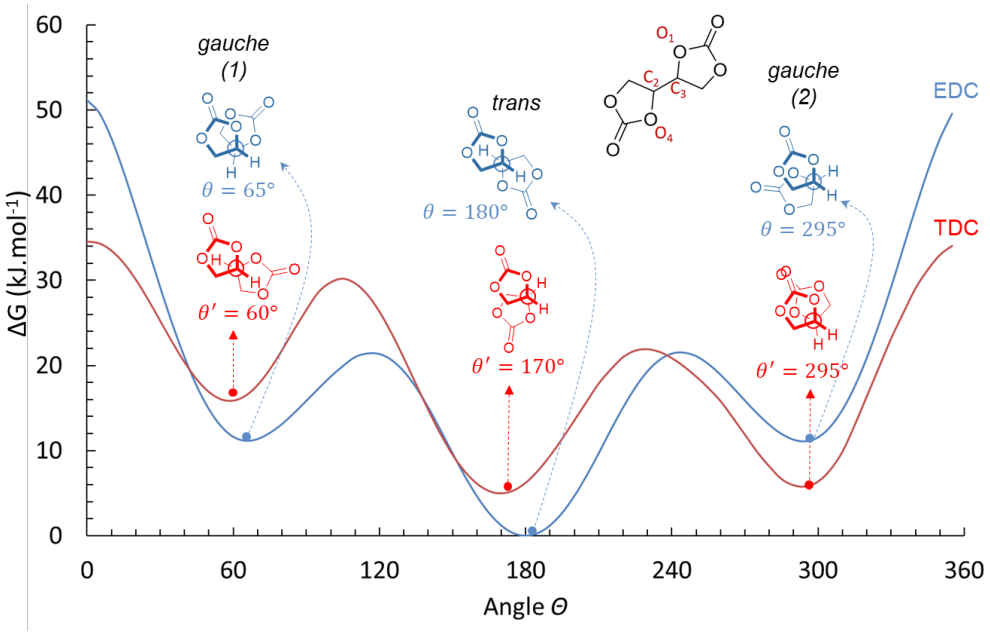

Figure 6: Energy levels of the conformers of EDC (blue plot) and TDC (red plot) in DMSO (1 mol.L^{-1}) at 25 °C, depending on the torsion angle, *Θ*, between the half-planes defined by O_1, C_3 and C_2 on one hand and O_4, C_2 and C_3 on the other hand.

The subsequent ring-opening aminolysis of the *in-situ* generated mixture of **1b** and **1b'** (95:5), was studied by adding an additional equivalent of HA. Again, the ^{1}H NMR monitoring of the reaction provides the second-order rate constant, $k_{2,TDC}$, of the second aminolysis reaction: $k_{2,TDC}$ = 0.064 L.mol^{-1}.h^{-1} (Supporting information: kinetics constant of EDC and TDC aminolysis, Figure S19). Interestingly, $k_{2,TDC} = k_{2,EDC}$, indicating that contrarily to the first aminolysis reaction, the kinetic rate of the second aminolysis is not impacted by the stereochemistry of the vicinal di(carbonate).

After completion of the second aminolysis reaction (4h, 60°C), the NMR analysis of the crude indicates that 64% of the overall hydroxyl groups are $(OH)_{II}$, and 36% are $(OH)_I$ (Supporting information: ^{1}H, ^{13}C, ^{1}H-^{1}H COSY and ^{1}H-^{13}C HSQC NMR spectra of all compounds, Figures S20 to S24). In that case, the ratio of the regiosiomers can be estimated to be **2b**:**2b'**:**2b''** = 30:65:5. Surprisingly, the regioselectivity of the second ring opening addition of TDC is inverted as compared to EDC. Indeed, NMR integrations indicate that 80% of the hydroxyl groups formed during the second ring opening reaction of TDC are $(OH)_I$, against 32% in the

case of EDC. These results suggest that the regioselectivity is significantly impacted by the stereochemistry. Magliozzi *et al*. already noticed a similar effect for the aminolysis of the different enantiomeric forms of DGDC, but to a lesser extent. Indeed, PHUs derived from the racemic mixture of *(R,R)* and *(S,S)* DGDC contain approximately 25% of $(OH)_I$ against 35% for PHUs derived from *meso*-DGDC. These results suggest that the conformational changes of the carbonates, from one stereoisomer to the other, impact not only the kinetics of their aminolysis, but also the orientation of the nucleophilic attack of the amine and thus the regioisomery of the resulting hydroxyurethane.

The mechanistic DFT calculation for the double ring opening aminolysis of TDC is presented in the Supplementary Information (Supporting information: ORCA calculations for TDC aminolysis, Figure S25). Similarly to EDC, the mechanistic pathways for the formation of the mono(hydroxyurethane)s, **1b-EA** and **1b'-EA**, indicates that the formation of **1b-EA**, the $(OH)_{II}$ containing regioisomer, is much more favorable under thermodynamic control ($\Delta\Delta G$(**1b'-EA**–**1b-EA**) = 32 kJ.mol^{-1}). The energy difference between the intermediary species, **IS1b**, and the transition state, **TS2b**, is essentially the same for the two regioisomers. Thus, the ratio **1b:1b'** = 95:5 is in accordance with the thermodynamic control of the reaction suggested by DFT calculation. When considering the energetic pathway for the formation of the di(hydroxyurethane)s **2b** and **2b'** (the formation of **2b''** is not considered here), the energy difference between the two regioisomers is small, $\Delta\Delta G$(**2b-EA**–**2b'-EA**) = 2 kJ.mol^{-1}, suggesting only a slight regioselectivity in favor of **2b'** formation, the regioisomer containing one $(OH)_{II}$ group and one $(OH)_I$ group. On the other hand, the energy difference between the intermediary species, **IS2b**, and the transition state, **TS4b**, indicate a slight regioselectivity in favor of **2b** formation. Thus, the experimental ratio, **2b**:**2b'**:**2b''** = 30:65:5, is in accordance with a thermodynamic control of the second aminolysis of TDC, despite the very small difference between the energy of the two regioisomers.

4. Synthesis of bis(cyclic carbonate) with different spacers

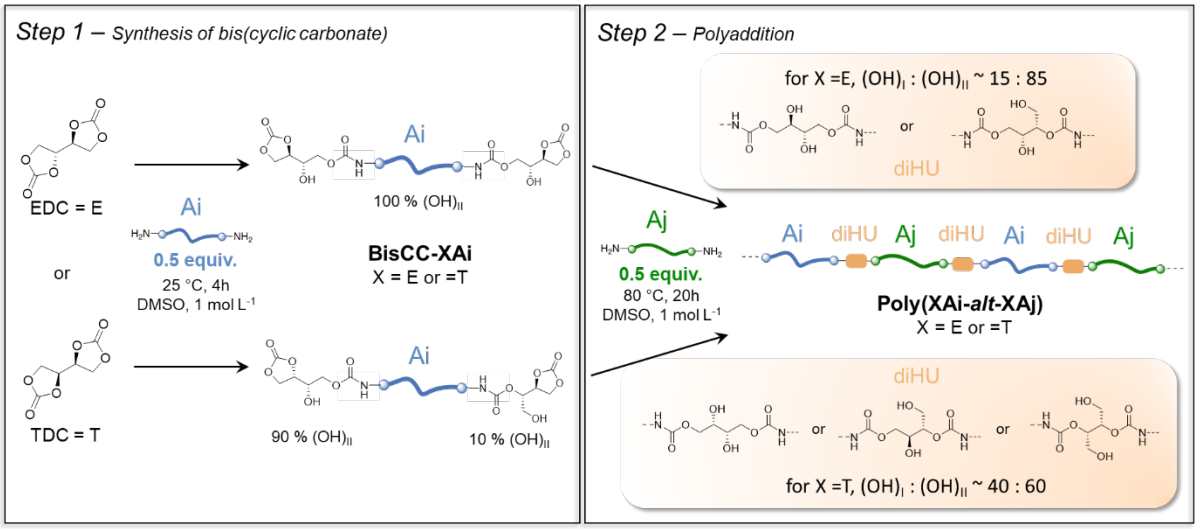

Figure 7: **The one-pot, two-step protocol for the synthesis of PHUs using the two vicinal dicarbonates, X = EDC or TDC. *Step 1*: Reaction of 1 equiv. of vicinal dicarbonate with 0.5 equiv. of a diamine, Ai, at 25 °C, to obtain a bis(cyclic carbonate), BisCC-XAi. *Step 2*: Reaction of BisCC-**

XAi with 0.5 equiv. of a diamine, Aj, at 60 °C, to obtain the corresponding PHUs, poly(XAi-*alt*-XAj).

By taking advantage of the remarkable difference of reactivity between the vicinal dicarbonates and their corresponding mono(hydroxyurethane)s in DMSO, PHUs synthesis was envisioned according to a one pot, two-step protocol. The principle, inspired from the results of the model reactions, is illustrated in Figure 7. It consists in, *step 1*, reacting 1 equiv. of vicinal dicarbonate with 0.5 equiv. of a diamine, **Ai**, at 25 °C, to obtain a bis(cyclic carbonate), **BisCC-XAi**, where X = E or T, with E standing for EDC and T for TDC, depending on the nature of the vicinal dicarbonate. Subsequently, in *step 2*, **BisCC-XAi** is reacted with an additional 0.5 equiv. of diamine, at 60 °C, to initiate a polyaddition reaction resulting in the formation of the corresponding PHUs. In *step 2*, the diamine can be the same as *step 1*, **Ai**, or a new diamine, **Aj**. In the latter case, the corresponding PHU is expected to have an alternated structure, ⋯**Ai-diHU-Aj-diHU**⋯, where **diHU** stands for di(hydroxyurethane)s. It is worth noting that a similar strategy was used by Ousaka *et al.* for the synthesis of sequence-controlled PHUs derived from a petroleum-based spiro bis(six-membered cyclic carbonate).[34] In their study, the **diHU** linkers were made of primary hydroxyl groups, $(OH)_I$, solely. In our case, the vicinal dicarbonates (EDC *vs* TDC) offer the additional possibility to tune the structure of the alcohols ($(OH)_I$ *vs* $(OH)_{II}$).

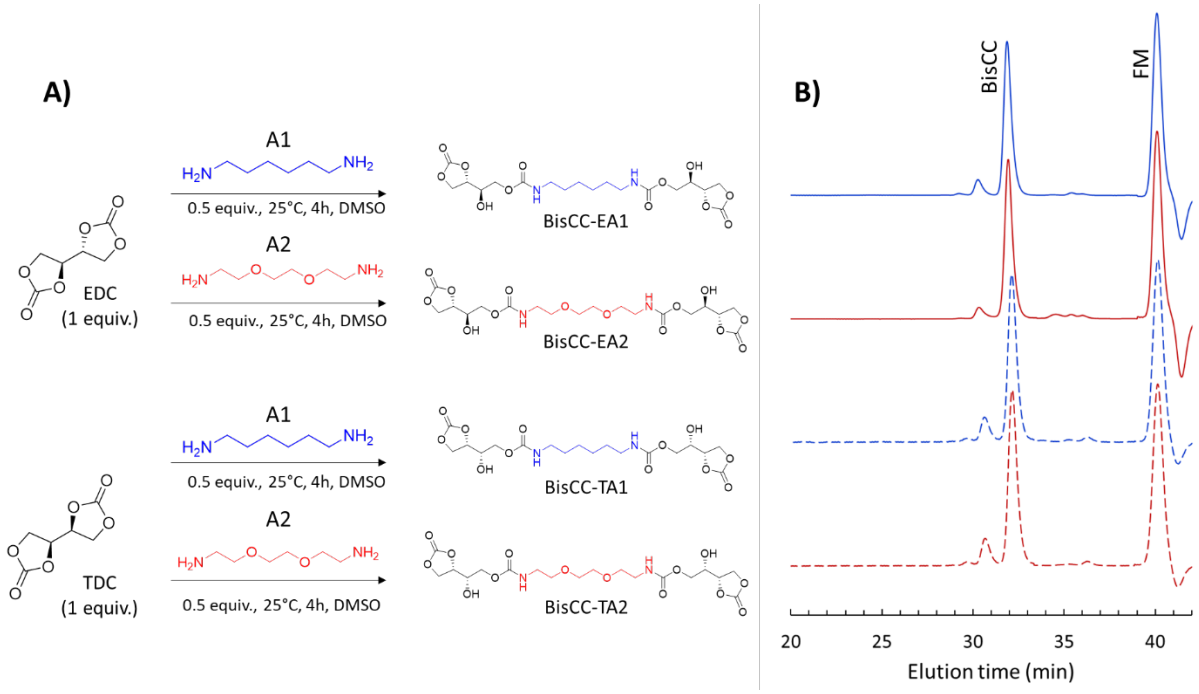

Figure 8: A) Syntheses of BisCC-XAi (X = E or T, i = 1 or 2) by reaction of EDC or TDC (1 equiv.) with diamines A1 or A2 (0.5 equiv.) at 25 °C for 4h in DMSO. B) SEC chromatograms of the corresponding BisCC-XAi (DMF + LiBr, calibration PS, FM: flow marker).

In this study, four **BisCC** precursors were synthesized by reacting EDC and TDC with two diamines: an aliphatic diamine **A1** = 1,6-Hexanediamine, and a short diether diamine **A2** = 1,8-diamino-3,6-dioxaoctane (Figure 8A). A typical synthesis proceeds by reacting 0.5 equiv. of EDC solubilized in DMSO (1 mol.L^{-1}) with 0.5 equiv. of **A1** at 25 °C for 4 h, to afford **BisCC-**

EA1. **BisCC-EA2**, **BisCC-TA1** and **BisCC-TA2** were successfully synthesized according to the same protocol. In all cases, the ^{1}H NMR characterization of the crudes indicates that the reaction is brought to completion. The conversions of CC are reported in Table 1. Moreover, NMR analysis was used to measure the $(OH)_I$: $(OH)_{II}$ ratios of the **BisCC**. For both **BisCC-EA1** and **BisCC-EA2**, $(OH)_I$: $(OH)_{II}$ = 0 : 100, in accordance with the model reaction of EDC with 1 equiv. of HA. For **BisCC-TA1**, and **BisCC-TA2**, $(OH)_I$: $(OH)_{II}$ ~ 10 : 90, again, in accordance with the model reaction of TDC with 1 equiv. of HA.

In order to validate the molecular structure of the **BisCCs** and to make sure that there is no oligomerization at this stage, the crudes were all analyzed by size exclusion chromatography (SEC). Figure 8B represents the chromatograms of all the **BisCCs**. In all cases, a sharp and intense peak is observed for an elution time, t_e ~ 32 min. The analysis of the peaks (Polystyrene calibration) provides number average molar masses, M_n, that are in close agreement with the theoretical molar masses of the BisCC. They are all reported in Table 1. The corresponding dispersity, $Đ$, are very close to 1, confirming the formation of well-defined **BisCC**.

It is worth noting that, on all chromatograms, a second peak is observed for an earlier elution time (t_e ~ 30.5 min). The corresponding M_n indicates the formation of **BisCC** dimers resulting from the reaction of two diamines with three vicinal dicarbonates. These dimers represent only 5% of the total mass of the samples. This small fraction is tolerated in the next part of the work. It implies that a known amount of **diHU-Ai-diHU-Ai-diHU** sequence will be inserted in the polymer synthesized from these crude **BisCCs**.

In the end, the difference of reactivity between the vicinal dicarbonates and their corresponding mono(hydroxyurethane)s in DMSO, enables the synthesis of well-defined **BisCC**, with good purity, and good control over the nature of the hydroxyl groups they contain. They can be used in *step 2*, as prepolymers for further polyaddition reaction with another diamine, **Aj**.

Table 1: Structural characteristics of BisCCs. [a] Conversions and $(OH)_I$: $(OH)_{II}$ ratios are measured by ^{1}H NMR spectroscopy of the crude samples. [b] M_n and $Đ$ are determined by SEC using a PS standard calibration and DMF with LiBr as eluant.

Vicinal carbonate	Diamine, **Ai**	BisCC	Conv.[a] (%)	$(OH)_I$: $(OH)_{II}$[a] (%)	M, Theoretical (g.mol^{-1})	M_n, SEC[b] (g.mol^{-1})	$Đ$[b]
EDC	A1	BisCC-EA1	> 99	0 : 100	464	550	1.05
EDC	A2	BisCC-EA2	> 99	0 : 100	496	560	1.03
TDC	A1	BisCC-TA1	> 99	9 : 91	464	540	1.07
TDC	A2	BisCC-TA2	> 99	10 : 90	496	540	1.08

5. One-pot synthesis of PHUs with tunable regioregularity

Polyhydroxyurethanes (PHU) were synthesized by polyaddition of the **BisCC** obtained according to the procedure described previously. To do so, 0.5 equiv. (to the initial amount of EDC or TDC) of amine **Aj** (where **j** = **i** = 1 or 2) were added to the *in-situ* generated **BisCC-XAi** (where **X** = E or T). Reactions were carried out at 80 °C for a period of 20 h. In all cases, the reaction is brought close to completion (conversions are reported in Table 2). The resulting polymers contain a simple repeating unit, **diHU-Ai**. They are denoted poly(**XAi**), where **X**

stands for the vicinal dicarbonate used in *step 1*, and **Ai** stands for the amine used in *step 1* and *step 2*.

The crude polymers were fully characterized by ^{1}H NMR spectroscopy and size exclusion chromatography. NMR spectroscopy was used to calculate the final CC conversion, which was further used to estimate the molar mass of the polymer according to the Carothers equation. The $(OH)_I$: $(OH)_{II}$ ratio were also calculated based on the NMR spectrum. The number average molar masses, M_n, and the dispersity, $Đ$, of the polymers were estimated *via* SEC measurements. Moreover, the thermal properties of the polymer were analyzed after solvent removal under high vacuum. The glass transition temperature, T_g, of the polymers and the heat capacity difference at T_g, ΔC_p, were measured by dynamic scanning calorimetry (DSC). Finally, their degradation temperature, $T_{d5\%}$ (temperature at 5 wt% loss) were measured by thermogravimetric analysis (TGA). The results are listed in Table 2.

Table 2 : Structural and thermal characteristics of the PHUs derived from erythritol and threitol dicarbonates. [a] Estimated by ^{1}H NMR spectroscopy analyses of the crude samples [b] Estimated by SEC using a PS standard calibration and DMF with LiBr as eluant. [c] Glass-transition temperature, T_g, and heat capacity difference at T_g, ΔCp, determined by differential scanning calorimetric analysis. [d] Temperature at 5 wt% loss determined by thermogravimetric analysis.

Vicinal dicarbonate	Diamine(s) 1st – 2nd	PHU	Conv.[a] (%)	$(OH)_I$: $(OH)_{II}$[a] (%)	M_{RMN}[a] (g.mol^{-1})	$M_{n,\,SEC}$[b] (g.mol^{-1})	$Đ$[b]	T_g[c] (°C)	ΔCp[c] ($mW.g^{-1}$)	$T_{d,5\%}$[d] (°C)
EDC	A1 – A1	Poly(EA1)	97.2	15 : 85	20 400	4 500	2.2	52	134	202
	A2 – A2	Poly(EA2)	95.8	14 : 86	15 000	3 560	2.8	25	104	206
	A1 – A2	Poly(EA1-alt-EA2)	95.2	19 : 81	12 400	2 310	2.5	24	124	205
	A2 – A1	Poly(EA2-alt-EA1)	96.5	17 : 83	17 200	3 780	3.2	27	110	204
	A1+A2	Poly(EA1-ran-EA2)	96.2	16 : 84	15 800	2 780	2.2	25	40	205
TDC	A1 – A1	Poly(TA1)	97.8	41 : 59	26 100	2 880	2.8	nd	nd	213
	A2 – A2	Poly(TA2)	96.7	40 : 60	19 200	2 770	2.9	8	11	210
	A1 – A2	Poly(TA1-alt-TA2)	98.3	43 : 57	35 700	4 120	3.7	10	63	214
	A2 – A1	Poly(TA2-alt-TA1)	98.6	43 : 57	43 400	4 640	4.6	20	46	211
	A1+A2	Poly(TA1-ran-TA2)	97.7	39 : 61	26 300	3 170	2.7	18	38	214

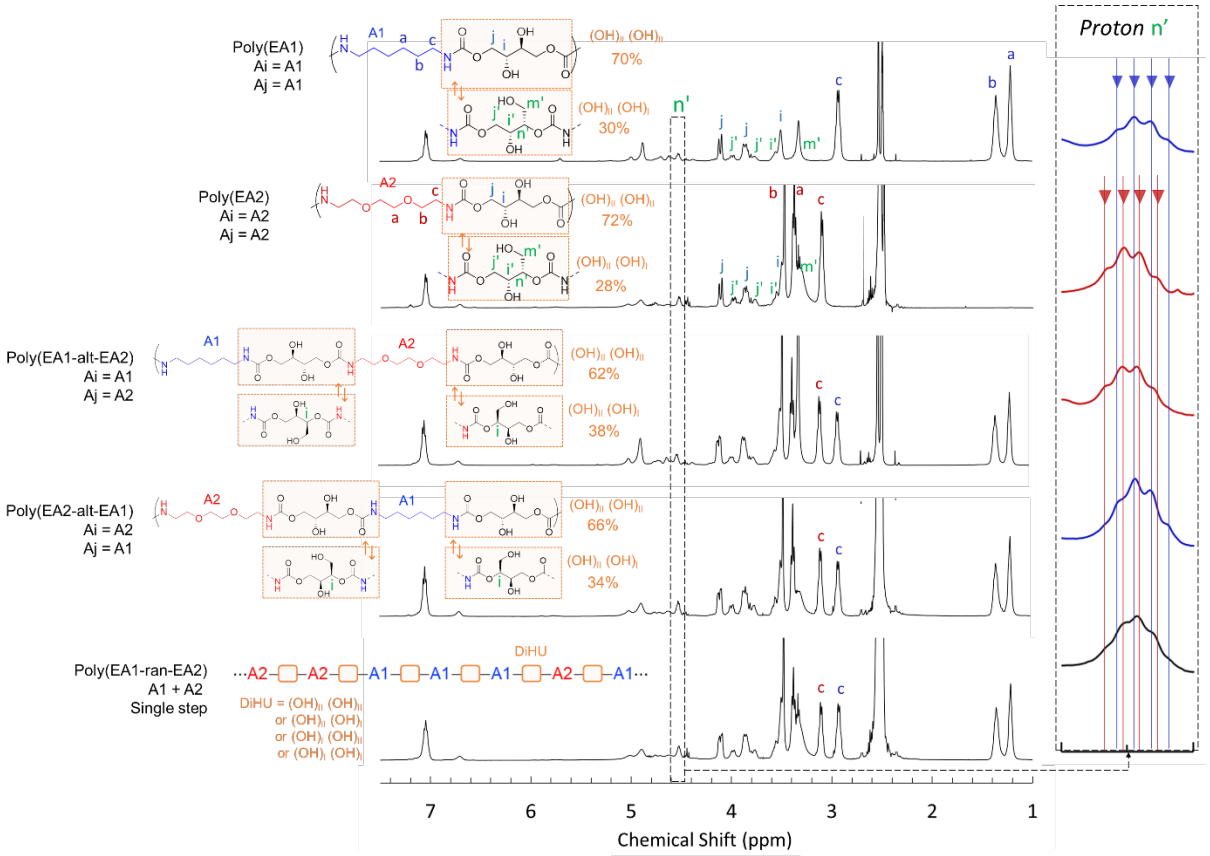

Figure 9: ^{1}H NMR characterization of the PHUs derived from EDC, *i.e.* from the reaction of BisCC-EAi (i = 1 or 2) with Aj (j = 1 or 2), at 80 °C for 20h (DMSO). For i = j: poly(EA1) and poly(EA2), for i ≠ j: poly(EA1-alt-EA2) and poly(EA2-alt-EA1). The NMR spectra of the homo- and alternated PHUs are compared to the NMR spectra of the random PHU obtained through the one-step reaction of EDC (1 equiv.) with a mixture of A1 (0.5 equiv.) and A2 (0.5 equiv.), poly(EA1-ran-EA2). The inset represents the magnification of the signal *n'* associated to the proton of the methine carbon of the primary hydroxyl groups.

The ^{1}H NMR spectra of poly(**EA1**) and poly(**EA2**) are presented in Figure 9. The conversion and thus the molar mass, M_{NMR}, are calculated by considering the signal at 4.79 ppm (proton of the methine carbon of end-chain carbonates): $M_{,NMR}$ = 20 400 g.mol^{-1} and 15 000 g.mol^{-1} for poly(**EA1**) and poly(**EA2**) respectively. The ratio $(OH)_I$: $(OH)_{II}$ are obtained by measuring the ratio of signals **j** (methyl protons of $(OH)_{II}$-$(OH)_{II}$ unit) and **j'**(methyl protons of $(OH)_{II}$-$(OH)_I$ unit) (Supporting information: ORCA calculations). We found $(OH)_I$: $(OH)_{II}$ = 15 : 85 and 16 : 84 for poly(**EA1**) and poly(**EA2**) respectively, in close agreement with the results obtained previously for the model reaction of EDC with HA. Thus, the regioselectivity of the second ring opening aminolysis of EDC is not impacted by the chain insertion process during the polyaddition reaction. The SEC traces of both polymers are plotted in Figure 10 (refractive index detector). Clearly, the chromatograms of the polymers are broad signals indicating the effective formation of polymers. At high elution time, the characteristic peak of **BisCC** almost disappeared, in agreement with its effective consumption. A series of sharp peaks with earlier elution time, reveals the presence of oligomers of low degree of polymerization. The analysis of the chromatogram using a conventional polystyrene calibration provides $M_{n,\,SEC}$ = 4 500 g.mol^{-1} and 3 560 g.mol^{-1} for poly(**EA1**) and poly(**EA2**) respectively. The evolutions of $M_{n,\,SEC}$

and M_{NMR} as a function of the amine **Ai** are consistent, but M_{NMR} is much larger than $M_{n,\,SEC}$ ($M_{NMR} \sim 4.5 \times M_{n,\,SEC}$). It must be stressed that the molar masses measured in SEC are based on a polystyrene calibration. Thus, $M_{n,\,SEC}$ are not the actual molar masses of the polymers. They can only be used to compare one polymer to another. Moreover, the hydroxyl groups of the polymers strongly interact with the columns of the SEC instrument (here poly(vinyl alcohol) columns). Therefore, $M_{n,\,SEC}$ are underestimated which might further explain the very large discrepancies between M_{NMR} and $M_{n,\,SEC}$. Some authors have circumvented this problem via the acetylation of the OH groups with acetic anhydride prior to the SEC measurement.[31]
The DSC thermograms of poly(**EA1**) and poly(**EA2**) are plotted in Figure 11A. T_g = 52 °C and 25 °C for poly(**EA1**) and poly(**EA2**) respectively. The T_g is much lower in the case of poly(**EA2**) because of the chain flexibility imparted by the ether backbone of **A2**.

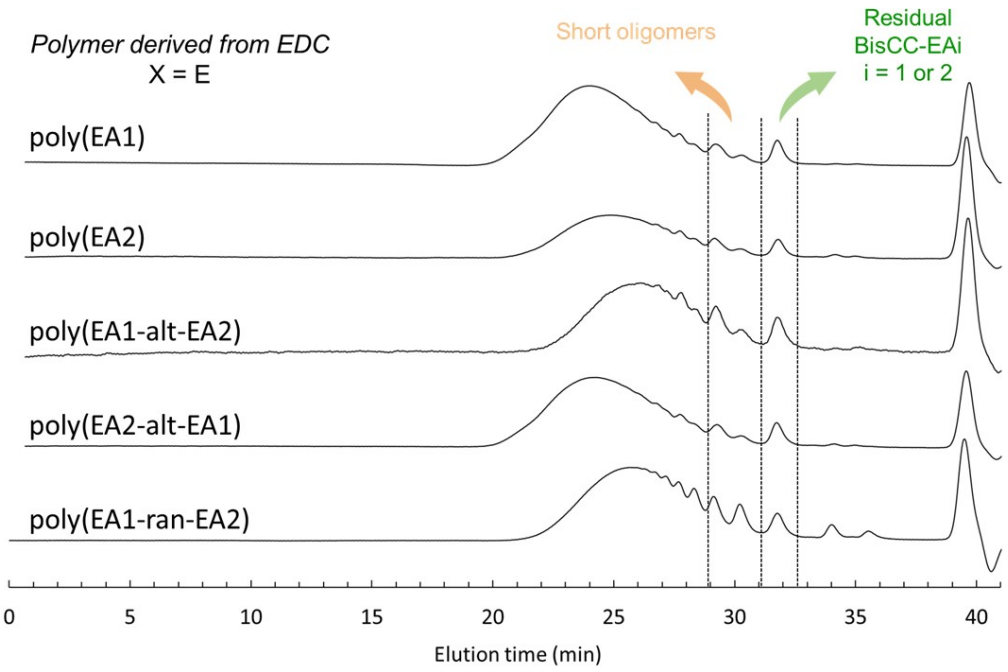

Figure 10: SEC chromatograms of poly(EA1), poly(EA2), poly(EA1-alt-EA2), poly(EA2-alt-EA1) and poly(EA1-ran-EA2). (DMF + LiBr, PS calibration)

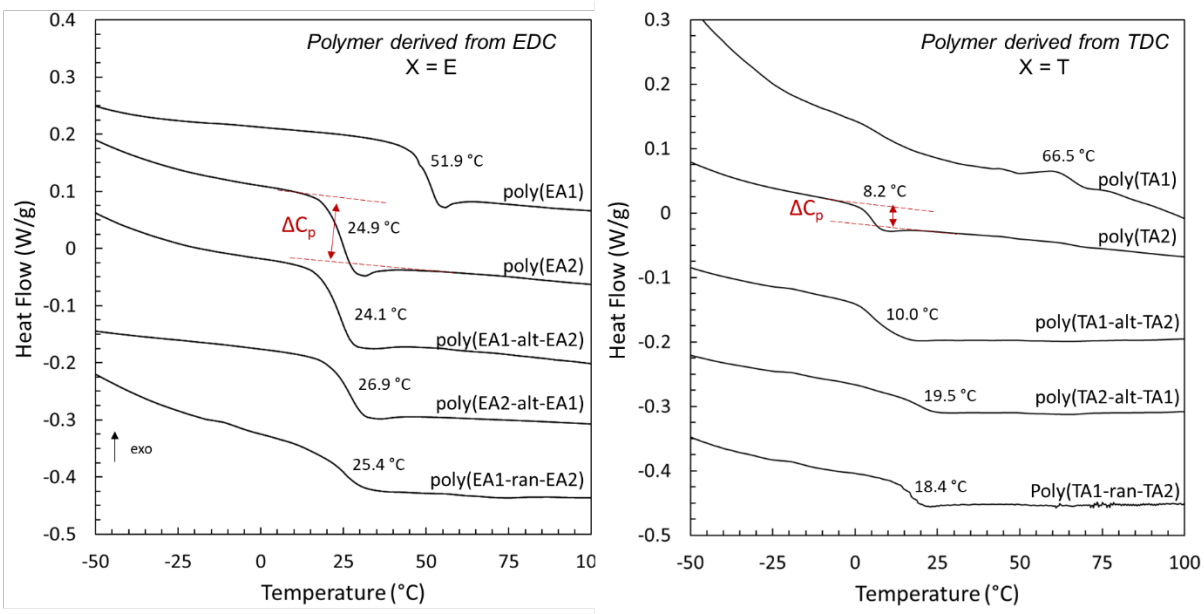

Figure 11: DSC thermograms of erythritol (left) and threitol (right) PHUs

The impact of the regioregularity onto the PHU's properties can be further investigated by considering the data collected for poly(**TA1**) and poly(**TA2**), the analogs of poly(**EA1**) and poly(**EA2**) obtained from TDC polymerization (Supporting information: ^{1}H NMR spectra and SEC traces of threitol PHUs, Figures S26 and S27). Indeed, NMR analyses indicate that M_{NMR} = 26 100 g.mol^{-1} and 19 200 g.mol^{-1}, and $(OH)_I$: $(OH)_{II}$ = 41 : 59 and 40 : 60 for poly(**TA1**) and poly(**TA2**) respectively. Again, the regioselectivity is in close agreement with the results obtained previously for the model reaction of TDC with HA. It is not impacted by the chain insertion process during the polyaddition reaction, suggesting that it is possible to synthesize PHUs with tunable regioregularity simply by tuning the stereochemistry of the vicinal dicarbonate. Indeed, the content of primary hydroxyl group is significantly increased when using TDC, the *(S,S)* stereoisomer, instead of EDC, its *(S,R)* diastereoisomer. With 85% of secondary hydroxyl groups, against 60% for the PHUs derived from TDC, the PHU derived from EDC exhibits a higher degree of regioregularity. The DSC thermograms of poly(**TA1**) and poly(**TA2**) are plotted in Figure 11B. When compared to the thermograms of poly(**EA1**) and poly(**EA2**), the most remarkable difference is that, the heat capacity difference at T_g, *i.e.* the difference of heat capacity between the glassy and the liquid state, ΔC_p, is much smaller in the case of poly(**TA1**) and poly(**TA2**). It is actually impossible to determine the T_g in the case of poly(**TA1**) because the thermogram exhibits several small variations of C_p with no indications enabling the identification of the actual glass transition. The T_g and ΔC_p of a polymer are clearly impacted by the number of inter- and intra-molecular hydrogen bonding of the polymer chains according to the literature.[35] Thus, it is not surprising that T_g and ΔC_p are dependent on $(OH)_I$: $(OH)_{II}$ for the PHUs synthesized in this work. T_g = 8 °C for poly(**TA2**) ($(OH)_I$: $(OH)_{II}$ = 40 : 60), against 25 °C for poly(**EA2**) ($(OH)_I$: $(OH)_{II}$ = 15 : 85). Again, this result suggests that the regioregularity of the PHUs has a direct impact on its thermal properties. The regioregularity of the PHUs being directly connected to the stereochemistry of the vicinal dicarbonates, our result suggest that it is possible, to some extent, to tune the thermal properties of PHUs by controlling the stereochemistry of the dicarbonates.

In our previous investigations of the impact of DGDC stereoisomery onto the microstructure of PHUs, only moderated variation of the T_g were observed between the PHUs obtained from the enantiopure *meso*-DGDC, *(R,S)*, *vs* the racemic mixture of *(R,R)* and *(S,S)* DGDC.[10] In this case, the variation of the hydroxyl ratio were of about 10%. For EDC *vs* TDC, we observe a two-fold increase of the magnitude of the variation (~ 20%), which might explain the larger variation of the thermal properties of the PHUs.

6. One-pot synthesis of alternated PHUs with tunable regioregularity

Alternated PHUs were synthesized by reacting 0.5 equiv. (to the initial amount of EDC or TDC) of amine **Aj**, where **j** = 1 or 2, with the *in-situ* generated **BisCC-XAi** , where **X** = E or T, **i** = 1 or 2 and **i ≠ j**. Reactions were carried out at 80 °C for a period of 20 h. In all cases, the reaction is brought close to completion (conversions are reported in Table 2). The resulting polymers are expected to contain the repeating unit **diHU-Ai-diHU-Aj** (cf. Figure 7). They are denoted poly(**XAi**-*alt*- **XAj**), where **X** stands for the vicinal dicarbonate used in *step 1*, **Ai** the amine used in *step 1* and **Aj** the amine used in *step 2*.

For comparison purposes, random copolymers were also synthesized according to a single step protocol: 1 equiv. of the vicinal dicarbonate (EDC or TDC) is mixed with 0.5 equiv. of amine **A1** and 0.5 equiv. of amine **A2**, in DMSO. The reaction is carried out at 25 °C for 4 h and 80 °C for 20 h. The random copolymers are denoted poly(**XA1**-*ran*- **XA2**), where **X** = E or T.
The crude PHUs were fully characterized according to the same methods (^{1}H NMR, SEC, DSC and TGA) and the resulting data are listed in Table 2.

The NMR spectra of Poly(**EA1**-*alt*-**EA2**), Poly(**EA2**-*alt*-**EA1**), and Poly(**EA1**-*ran*-**EA2**) are plotted in Figure 9. Their corresponding molar masses, M_{RMN}, and $(OH)_I$: $(OH)_{II}$ ratios are reported in Table 2. They are of the same order of magnitude than Poly(**EA1**) and Poly(**EA2**). As expected, the copolymerization with a second diamine, **Aj**, different than **Ai**, offers the same control over the regioregularity of the resulting polymer. The inset of Figure 9 represents a magnification of the signal **n'**, associated to the proton of the methine carbon of the primary hydroxyl groups, $(OH)_I$. The shape and the multiplicity of this signal are very similar for Poly(**EA1**) and Poly(**EA2**-*alt*-**EA1**). The same observation is true for Poly(**EA2**) and Poly(**EA1**-*alt*-**EA2**). On the other hand, the signal of Poly(**EA1**-*ran*-**EA2**) looks like a combination of the signals of Poly(**EA1**) and Poly(**EA2**). Knowing that $(OH)_I$ are exclusively formed during *step 2*, *i.e.* the polyaddition reaction of **Aj**, with **BisCC-EAi** (**i ≠ j**), it is expected that, in the resulting polymer Poly(**EAi**-*alt*-**EAj**), the proton of the methine carbon **n'** are essentially (de)shieldied by the amine **Aj**, just like in Poly(**EAj**). Thus, the resemblance of the signals of the proton **n'** of Poly(**EAj**) and Poly(**EAi**-*alt*-**EAj**) is expected. It is an indirect evidence in favor of the alternated structure of Poly(**EA1**-*alt*-**EA2**) and Poly(**EA2**-*alt*-**EA1**). It is worth noting that, due to the low resolution of the NMR spectra, high-field NMR spectroscopy would be necessary to further confirm this interpretation.
The SEC chromatograms of the alternated and the random PHUs are presented in Figure 10. The corresponding number average molar masses, $M_{n,\,SEC}$, are reported in Table 2. Again M_{NMR}

~ 5×$M_{n,\,SEC}$, reflecting the underestimation of the molecular weights in SEC chromatography. The DSC thermograms are plotted in Figure 11. T_g = 24 °C and 27 °C for Poly(**EA1**-*alt*-**EA2**) and Poly(**EA2**-*alt*-**EA1**) respectively, indicating that the addition order of the two amines **Ai** (**i** = 1 or 2), does not impact the thermal properties of the polymer significantly. Moreover, T_g = 25 °C for Poly(**EA1**-*ran*-**EA2**), suggesting that the thermal properties of these PHUs are essentially dependent on the structure of the diamine residues and almost independent of the sequence regularity. This was also the case for the sequenced-controlled PHUs derived from the symmetric spiro bis(six-membered cyclic carbonate) of Ousaka and Endo.[34]

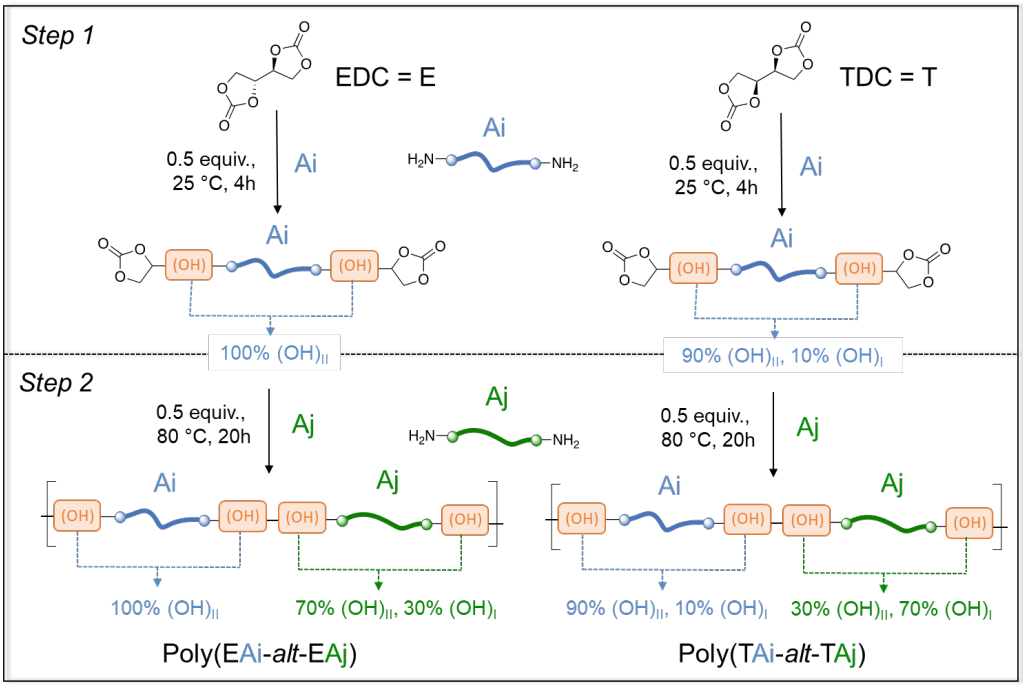

Figure 12: Schematic representations of the structural composition of the biscarbonates, BisCC-XAi, derived from the reaction of EDC or TDC (X = E or T) with the diamine Ai (i = 1 or 2) (25 °C, 4 h, DMSO), and of the corresponding PHUs derived from the reaction of BisCC-XAi with the diamine Aj (j = 1 or 2), poly(XAi-*alt*- XAj) (80 °C, 20 h, DMSO). The schemes indicate the $(OH)_I$: $(OH)_{II}$ ratios for the neighboring hydroxyl groups of the Ai and the Aj segments.

The results obtained for Poly(**TA1**-*alt*-**TA2**), Poly(**TA2**-*alt*-**TA1**), and Poly(**TA1**-ran-**TA2**), (see Table 2) indicate that their regioregularity is in accordance with those of the homopolymers Poly(**TA1**), and Poly(**TA2**): $(OH)_I$: $(OH)_{II}$ ~ 40 : 60, against 15 : 85 for their analogs derived from EDC. Therefore, it is possible to tune the regioregularity of the sequence-controlled PHUs derived from vicinal dicarbonates by playing with the stereochemistry of the cyclic carbonates. The DSC thermograms of Poly(**TA1**-*alt*-**TA2**), Poly(**TA2**-*alt*-**TA1**), and Poly(**TA1**-ran-**TA2**) are plotted in Figure 11. Again, the heat capacity difference at T_g, ΔC_p, is much smaller than those of their EDC-analogs, suggesting an impact of the regioregularity on the intra- and the inter-molecular interactions of the polymers. Moreover, contrarily to their EDC-analogs, there is a noticeable influence of the addition order of the amines onto the T_g of the sequence-controlled PHUs. Indeed, T_g = 10 °C and 20 °C for Poly(**TA1**-*alt*-**TA2**) and Poly(**TA2**-*alt*-**TA1**) respectively. This result suggests that the positioning of the amine surrogate as compared

to the primary hydroxyl groups, $(OH)_I$, essentially generated during *step 2*, has an impact on the T_g of the polymers. Figure 12 recaps the nature of the neighboring (OH) groups of the **Ai** and the **Aj** segments respectively, as a function of the addition order of the diamines, for both EDC and TDC. For TDC, when **Aj** = **A2** (*step 2)*, the oxygen of the ether linkages of **A2** can easily interact with the pendant $(OH)_I$, *via* intra-molecular hydrogen bonding. Figure 13 represents one possible chain conformation resulting in the formation of such intra-molecular arrangements. This can presumably lead to an increase of the number of intra-molecular interactions, at the expense of the inter-molecular arrangements, and thus, to a decrease of the T_g. On the contrary, when **Ai** =**A2** (*step 1)*, the intra-molecular distance between $(OH)_I$ and the ether linkages increases. In this case, the closest (OH) neighbors of **A2** are the hindered secondary hydroxyl groups generated during *step 1*, $(OH)_{II}$, which might be less accessible to develop hydrogen bonding with the ether linkages of **A2**. When EDC is used, instead of TDC, there are much less $(OH)_I$ generated during *step 2*. This might explain why the addition order of the amine has less impact on the T_g of the polymers in this case. In the end, this last result suggest that it is possible to tune the thermal properties of these sequence-controlled PHUs by playing both with their sequence- and regio-regularity.

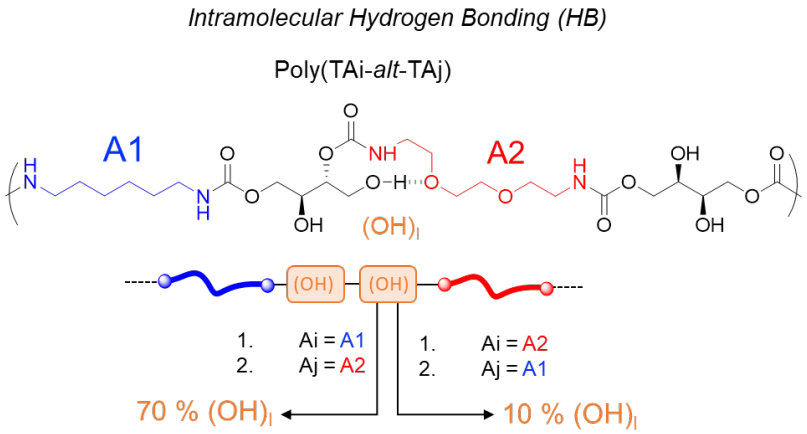

Figure 13: Schematic representation of the intramolecular hydrogen bonding between the oxygen atom of the ethers of A2 and the primary hydroxyl groups, $(OH)_I$, of the adjacent dihydroxyurethane linker, within the backbone of the alternated PHUs, Poly(TAi-*alt*-TAj) (i ≠ j). Relative proportions of $(OH)_I$ (vs $(OH)_{II}$) directly adjacent to A2 oxygen depending on the addition order of A1 and A2 during the one-pot, two-step synthesis of Poly(TAi-*alt*-TAj) (i ≠ j). Right, 10%: A2 is added during *step 1*, Left, 70%: A2 is added during *step 2*.

Conclusion

In conclusion, we have explained the high reactivity of vicinal dicarbonates (EDC and TDC) and demonstrated that this reactivity is highly suitable for the synthesis of well-defined novel di(hydroxy-urethane) dicarbonates (BisCC) in soft experimental conditions (25 °C, ambient atmosphere, 4 h). The selectivity of the hydroxyl group obtained during the ring opening reaction of cyclic carbonate is dictated by the spatial configuration of EDC and TDC. $BisCC_2$ with $(OH)_{II}$-$(OH)_{II}$ groups are obtained from two diamines under the same experimental

condition and with similar selectivity. This result opens the possibility to design a new platform of bio-based 5CCs. Moreover, macromolecular engineering allows the creation of regioregular PHUs, with tuneable and controllable properties, using sustainable products, such as sugar derivative tetraols. A broad range of properties can be obtained from erythritol and threitol-based PHUs, by a very simple selection of diamines and vicinal 5CCs. These simple way of synthesis of poly(hydroxy-urethane)s is promising in order to obtain green and functional polymers at low cost to respond to nowadays challenges.

Associated content

Additional experimental details, materials, and methods, crystallographic parameters and DSC traces of EDC and TDC, NMR characterizations of all compounds, ORCA calculations for the aminolysis of all carbonate compounds.

Author Information

Corresponding authors: Henri Cramail (cramail@enscbp.fr); Etienne Grau (egrau@enscbp.fr); Thomas Vidil (thomas.vidil@enscbp.fr)

Notes: The authors declare no competing financial interest

Acknowledgements

The authors are grateful for financial support from PolymerExpert and ANRT. The authors thank Brice Kauffmann (IECB, University of Bordeaux) for single-crystal X-ray analysis.

A preprint of this manuscript has been published in ChemRxiv : https://doi.org/10.26434/chemrxiv-2022-m5fv2

References

(1) Maisonneuve, L.; Lamarzelle, O.; Rix, E.; Grau, E.; Cramail, H. Isocyanate-Free Routes to Polyurethanes and Poly(hydroxy Urethane)s. *Chem. Rev.* **2015**, *115* (22), 12407-12439.

(2) Carré, C.; Ecochard, Y.; Caillol, S.; Avérous, L. From the Synthesis of Biobased Cyclic Carbonate to Polyhydroxyurethanes: A Promising Route towards Renewable Non-Isocyanate Polyurethanes. *ChemSusChem* **2019**, *12* (15), 3410-3430.

(3) Grignard, B.; Gennen, S.; Jérôme, C.; Kleij, A. W.; Detrembleur, C. Advances in the use of CO2 as a renewable feedstock for the synthesis of polymers. *Chem. Soc. Rev.* **2019**, *48* (16), 4466-4514.

(4) Yadav, N.; Seidi, F.; Crespy, D.; D'Elia, V. Polymers Based on Cyclic Carbonates as Trait d'Union Between Polymer Chemistry and Sustainable CO 2 Utilization. *ChemSusChem* **2018**, *12* (4), 724-754.

(5) Alves, M.; Grignard, B.; Mereau, R.; Jerome, C.; Tassaing, T.; Detrembleur, C.

Organocatalyzed coupling of carbon dioxide with epoxides for the synthesis of cyclic carbonates: Catalyst design and mechanistic studies. *Catal. Sci. Technol.* **2017**, *7* (13), 2651-2684.

(6) Alves, M.; Grignard, B.; Gennen, S.; Detrembleur, C.; Jerome, C.; Tassaing, T. Organocatalytic synthesis of bio-based cyclic carbonates from CO2 and vegetable oils. *RSC Adv.* **2015**, *5* (66), 53629-53636.

(7) Aomchad, V.; Cristòfol, À.; Della Monica, F.; Limburg, B.; D'Elia, V.; Kleij, A. W. Recent progress in the catalytic transformation of carbon dioxide into biosourced organic carbonates. *Green Chem.* **2021**, *23* (3), 1077-1113.

(8) Dannecker, P.-K.; Meier, M. A. R. Facile and Sustainable Synthesis of Erythritol bis(carbonate), a Valuable Monomer for Non-Isocyanate Polyurethanes (NIPUs). *Nat. Sci. Reports* **2019**, *9:9858,* 1-6.

(9) Magliozzi, F.; Chollet, G.; Grau, E.; Cramail, H. Benefit of the Reactive Extrusion in the Course of Polyhydroxyurethanes Synthesis by Aminolysis of Cyclic Carbonates. *ACS Sustain. Chem. Eng.* **2019**, *7*, 17282-17292.

(10) Magliozzi, F.; Scali, A.; Chollet, G.; Grau, E.; Cramail, H. Enantioselective Crystallization of Diglycerol Dicarbonate: Impact of the Microstructure on Polyhydroxyurethane Properties. *Macromol. Rapid Commun.* **2021**, *42* (3), 1-9.

(11) Bobbink, F. D.; Van Muyden, A. P.; Dyson, P. J. En route to CO2-containing renewable materials: Catalytic synthesis of polycarbonates and non-isocyanate polyhydroxyurethanes derived from cyclic carbonates. *Chem. Commun.* **2019**, *55* (10), 1360-1373.

(12) Zhou, H.; Zhang, H.; Mu, S.; Zhang, W. Z.; Ren, W. M.; Lu, X. B. Highly regio- And stereoselective synthesis of cyclic carbonates from biomass-derived polyols: Via organocatalytic cascade reaction. *Green Chem.* **2019**, *21* (23), 6335-6341.

(13) Ecochard, Y.; Caillol, S. Hybrid polyhydroxyurethanes: How to overcome limitations and reach cutting edge properties? *Eur. Polym. J.* **2020**, *137* (109915), 1-21.

(14) Blain, M.; Cornille, A.; Boutevin, B.; Auvergne, R.; Benazet, D.; Andrioletti, B.; Caillol, S. Hydrogen bonds prevent obtaining high molar mass PHUs. *J. Appl. Polym. Sci.* **2017**, *134* (45), 1-23.

(15) Lamarzelle, O.; Durand, P. L.; Wirotius, A. L.; Chollet, G.; Grau, E.; Cramail, H. Activated lipidic cyclic carbonates for non-isocyanate polyurethane synthesis. *Polym. Chem.* **2016**, *7* (7), 1439-1451.

(16) Gennen, S.; Grignard, B.; Tassaing, T.; Jérôme, C.; Detrembleur, C. CO 2 -Sourced α-Alkylidene Cyclic Carbonates: A Step Forward in the Quest for Functional Regioregular Poly(urethane)s and Poly(carbonate)s . *Angew. Chemie* **2017**, *129* (35), 10530-10534.

(17) Lombardo, V. M.; Dhulst, E. A.; Leitsch, E. K.; Wilmot, N.; Heath, W. H.; Gies, A. P.; Miller, M. D.; Torkelson, J. M.; Scheidt, K. A. Cooperative catalysis of cyclic carbonate ring opening: Application towards non-isocyanate polyurethane materials. *European J. Org. Chem.* **2015**, 2791-2795.

(18) Blain, M.; Yau, H.; Jean-Gérard, L.; Auvergne, R.; Benazet, D.; Schreiner, P. R.; Caillol, S.; Andrioletti, B. Urea-and thiourea-catalyzed aminolysis of carbonates. *ChemSusChem* **2016**, *9* (16), 2269-2272.

(19) Chile, L. E.; Mehrkhodavandi, P.; Hatzikiriakos, S. G. A Comparison of the Rheological and Mechanical Properties of Isotactic, Syndiotactic, and Heterotactic Poly(lactide). *Macromolecules* **2016**, *49* (3), 909-919.

(20) De Rosa, C.; Auriemma, F.; De Ballesteros, O. R.; Resconi, L.; Camurati, I. Tailoring the physical properties of isotactic polypropylene through incorporation of comonomers and the precise control of stereo-and regioregularity by metallocene catalysts. *Chem. Mater.* **2007**, *19* (21), 5122-5130.

(21) Kim, Y.; Park, H.; Park, J. S.; Lee, J. W.; Kim, F. S.; Kim, H. J.; Kim, B. J. Regioregularity-control of conjugated polymers: From synthesis and properties, to photovoltaic device applications. *J. Mater. Chem. A* **2022**, *10* (6), 2672-2696.

(22) Stubbs, C. J.; Worch, J. C.; Prydderch, H.; Wang, Z.; Mathers, R. T.; Dobrynin, A. V.; Becker, M. L.; Dove, A. P. Sugar-Based Polymers with Stereochemistry-Dependent Degradability and Mechanical Properties. *J. Am. Chem. Soc.* **2022**, *144* (3), 1243-1250.

(23) Tomita, H.; Sanda, F.; Endo, T. Model reaction for the synthesis of polyhydroxyurethanes from cyclic carbonates with amines: Substituent effect on the reactivity and selectivity of ring-opening direction in the reaction of five-membered cyclic carbonates with amine. *J. Polym. Sci. Part A Polym. Chem.* **2001**, *39* (21), 3678-3685.

(24) Ochiai, B.; Koda, K.; Endo, T. Branched cationic polyurethane prepared by polyaddition of chloromethylated five-membered cyclic carbonate and diethylenetriamine in molten salts. *J. Polym. Sci. Part A Polym. Chem.* **2012**, *50*, 47-51.

(25) Iwasaki, T.; Kihara, N.; Endo, T. Reaction of various oxiranes and carbon dioxide. Synthesis and aminolysis of five-membered cyclic carbonates. *Bull. Chem. Soc. Jpn* **2000**, *73*, 713-719.

(26) Sopeña, S.; Laserna, V.; Guo, W.; Martin, E.; Escudero-Adán, E. C.; Kleij, A. W. Regioselective Organocatalytic Formation of Carbamates from Substituted Cyclic Carbonates. *Adv. Synth. Catal.* **2016**, *358* (13), 2172-2178.

(27) Muzyka, C.; Monbaliu, J.-C. Perspectives for the Upgrading of Bio-Based Vicinal Diols within the Developing European Bioeconomy. *ChemSusChem* **2022**, *15* (5), e202102391.

(28) Goldstein, B. N.; Goryunov, A. N.; Gotlib, Y. Y.; Elyashevich, A. M.; Zubova, T. P.; Koltzov, A. I.; Nemirovskii, V. D.; Skorokhodov, S. S. Investigation of cooperative kinetics on reactions of functional groups on polymer chains. *J. Polym. Sci. Part A-2 Polym. Phys.* **1971**, *9* (5), 769-777.

(29) Meyer, H. R. Dicarbonate und Dicarbamate des DL-Threits und des Erythrits. **1966**, *49* (6), 1935-1937.

(30) Whelan, J. M.; Hill, M.; Sam, W. P. Multiple cyclic carbonate polymers from erythritol

dicarbonate, US2935494 (A), in United States Patents Office, U.C. Corporation, 1960.

(31) Schmidt, S.; Gatti, F. J.; Luitz, M.; Ritter, B. S.; Bruchmann, B.; Mülhaupt, R. Erythritol Dicarbonate as Intermediate for Solvent- and Isocyanate-Free Tailoring of Bio-Based Polyhydroxyurethane Thermoplastics and Thermoplastic Elastomers. *Macromolecules* **2017**, *50*, 2296-2303.

(32) Li, L.; Zhao, B.; Wang, H.; Gao, Y.; Hu, J.; Zheng, S. Nanocomposites of polyhydroxyurethane with Fe3O4 nanoparticles: Synthesis, shape memory and reprocessing properties. *Compos. Sci. Technol.* **2021**, *215* (109009), 1-8.

(33) Schmidt, S.; Ritter, B. S.; Kratzert, D.; Bruchmann, B.; Mülhaupt, R. Isocyanate-free route to poly(carbohydrate-urethane) thermosets and 100% bio-based coatings derived from glycerol feedstock. *Macromolecules* **2016**, *49* (19), 7268-7276.

(34) Ousaka, N.; Endo, T. One-Pot Nonisocyanate Synthesis of Sequence-Controlled Poly(hydroxy urethane)s from a Bis(six-membered cyclic carbonate) and Two Different Diamines. *Macromolecules* **2021**, *54* (5), 2059-2067.

(35) Hatakeyama, T.; Hatakeyama, H. Effect of chemical structure of amorphous polymers on heat capacity difference at glass transition temperature. *Thermochim. Acta* **1995**, *267*, 249-257.